

Alma Mater Studiorum Università di Bologna
Archivio istituzionale della ricerca

Morphological description and morphometric analyses of the Upper Palaeolithic human remains from Dzudzuana and Satsurblia caves, western Georgia

This is the final peer-reviewed author's accepted manuscript (postprint) of the following publication:

Published Version:

Margherita, C., Oxilia, G., Barbi, V., Panetta, D., Hublin, J., Lordkipanidze, D., et al. (2017). Morphological description and morphometric analyses of the Upper Palaeolithic human remains from Dzudzuana and Satsurblia caves, western Georgia. JOURNAL OF HUMAN EVOLUTION, 113, 83-90 [10.1016/j.jhevol.2017.07.011].

Availability:

This version is available at: <https://hdl.handle.net/11585/610332> since: 2018-10-09

Published:

DOI: <http://doi.org/10.1016/j.jhevol.2017.07.011>

Terms of use:

Some rights reserved. The terms and conditions for the reuse of this version of the manuscript are specified in the publishing policy. For all terms of use and more information see the publisher's website.

This item was downloaded from IRIS Università di Bologna (<https://cris.unibo.it/>).
When citing, please refer to the published version.

(Article begins on next page)

This is the final peer-reviewed accepted manuscript of:

Margherita C, Oxilia G, Barbi V, Panetta D, Hublin JJ, Lordkipanidze D, Meshveliani T, Jakeli N, Matskevich Z, Bar-Yosef O, Belfer-Cohen A, Pinhasi R, Benazzi S.

Morphological description and morphometric analyses of the Upper Palaeolithic human remains from Dzudzuana and Satsurbliia caves, western Georgia, *J. Hum. Evol.* 113, 83–90 (2017).

The final published version is available online at:

<https://doi.org/10.1016/j.jhevol.2017.07.011>

© 2017. This manuscript version is made available under the Creative Commons Attribution-NonCommercial-NoDerivatives (CC BY-NC-ND) License 4.0 International
(<http://creativecommons.org/licenses/by-nc-nd/4.0/>)

Morphological description and morphometric analyses of the Upper Palaeolithic human remains from Dzudzuana and Satsurblia caves, western Georgia

Cristiana Margherita¹, Gregorio Oxilia^{1,2}, Veronica Barbi¹, Daniele Panetta³, Jean – Jacques Hublin⁴, David Lordkipanidze⁵, Tengiz Meshveliani⁵, Nino Jakeli⁵, Zinovi Matskevich⁶, Ofer Bar-Yosef⁷, Anna Belfer-Cohen⁸, Ron Pinhasi^{9,10*}, Stefano Benazzi^{1,4*}

¹*Department of Cultural Heritage, University of Bologna, Via degli Ariani 1, 48121 Ravenna, Italy*

²*Department of Biology, University of Florence, Via del Proconsolo 12, 50122 Firenze, Italy*

³*Institute of Clinical Physiology – CNR, Pisa, Italy*

⁴*Department of Human Evolution, Max Planck Institute for Evolutionary Anthropology, Deutscher Platz 6, 04103 Leipzig, Germany*

⁵*Georgian National Museum, Department of Prehistory, Tbilisi, Georgia*

⁶*Israel Antiquities Authority, Jerusalem, Israel*

⁷*Department of Anthropology, Peabody Museum, Harvard University, 11 Divinity Avenue, Cambridge, MA 02138, USA*

⁸*The Institute of Archaeology, The Hebrew University of Jerusalem, Mount Scopus, Jerusalem 91905, Israel*

⁹*School of Archaeology and Earth Institute, University College Dublin, Belfield, Dublin 4, Ireland*

¹⁰*Department of Anthropology, University of Vienna, Althanstrasse 14, 1090 Vienna, Austria*

*Corresponding author.

E-mail address: ron.pinhasi@ucd.ie; stefano.benazzi@unibo.it

Keywords: *Homo sapiens*; teeth; mandible; Late Pleistocene; digital analyses; 3D enamel thickness

Introduction

While paleoanthropologists and archaeologists agree that western Georgia was used as a thoroughfare of human movements to and from the Caucasus (Pinhasi et al., 2012, 2014), the paleoanthropological fossil record of the local Middle and Upper Palaeolithic in this key region is currently limited to scant human remains. For the Late Pleistocene, the Middle Palaeolithic (MP) Georgian human fossil record consists of a partial maxilla from the site of Sakajia and some isolated teeth from the sites of Bronze Cave, Djruchula, Ortvala and Ortvale Klde, which were all classified as Neandertals (Pinhasi et al., 2012). The Upper Palaeolithic (UP) fossil record consists of a modern human tooth from Bondi cave (Tushabramishvili et al., 2012), recently dated between 39,000 and 35,800 cal. BP (calibrated years before present; Pleurdeau et al., 2016), and cranial fragments from Sakajia, dated between 12,000 and 10,000 cal. BP (Nioradze and Otte, 2000) (Supplementary Online Material [SOM] Fig. S1). Therefore, even though some authors suggests that the Caucasus represents a sort of cul de sac for Neandertal survival, and that modern humans arrived in this area much later compared to other regions (Bar-Yosef and Pilbeam, 2000), the paucity of human remains prevents any conclusive assessment.

Here we report additional Upper Palaeolithic human remains from the Imereti region, western Georgia (SOM Fig. S1): two isolated teeth from Dzudzuana cave, Dzu 1 and Dzu 2 (both deciduous; Bar-Yosef et al., 2011), and one isolated tooth (SATP5-2, deciduous) and a hemi-mandible (SATP5) bearing permanent and deciduous teeth (SATP5-3 – SATP5-7) from Satsurbliia cave (Pinhasi et al., 2014). In particular, the human remains from Dzudzuana cave, dated between 27,000 and 24,000 cal. BP, fill a huge gap in the Upper Palaeolithic Georgian fossil record and play an important role in the debate about modern human peopling of the Caucasus.

Materials and methods

Micro-CT

High-resolution μ CT images of the teeth from Dzudzuana (Dzu 1 and Dzu 2; Fig. 1) and the isolated tooth from Satsurbliia (SATP5-2) (Fig. 2) were obtained with a XALT microtomographic system (Institute of Clinical Physiology, Pisa, Italy) (Panetta et al., 2012). The Satsurbliia mandible (Fig. 3) was scanned with a Birscan microtomographic system (Max Planck Institute for Evolutionary Anthropology, Leipzig, Germany); scan parameters and processing procedures are described in the SOM (SOM Fig S2, S3).

Morphological description

Terminology for the morphological description of the mandible and the teeth follows White et al. (2012) and Scott and Turner (1997), respectively. Nonmetric traits were evaluated according to standards outlined by the Arizona State University Dental Anthropology System (ASUDAS; Turner et al. [1991], Bailey [2002], Bailey et al. [2011] and Martínez de Pinillos et al. [2014]). Occlusal wear stage was assessed based on Molnar (1971). For deciduous teeth, the age at death was estimated combining different observations, such as stages of tooth formation, dental eruption and root resorption using the sequences provided by Moorrees (1963) and Al Qahtani and colleagues (2010).

Morphometric analyses

Height and breadth of the mandibular corpus were measured in the digital model at the level of both the mental foramen (Buikstra and Ubelaker, 1994) and the lower first molar (Rosas and Bermúdez de Castro, 1999). For the deciduous molars, we measured mesiodistal (MD) and buccolingual (BL) crown diameters (Benazzi et al., 2011a; 2013a; Margherita et al., 2016), and we used crown (for Dzu 1, Dzu 2 and SATP5-5) and cervical outline analyses (for Dzu 2 and SATP5-5), following methods described in Benazzi et al. (2011b; 2012a; 2014a) and Bailey et al. (2014). For the permanent teeth (but not for the deciduous teeth, which are heavily worn), we computed three-dimensional (3D) enamel thickness following guidelines provided by Benazzi and

colleagues (2014b). Finally, to assess whether Dzu 1 and Dzu 2 belong to the same individual, both teeth were analysed using the Occusal Fingerprint Analyser (OFA) software package (2008-2014 ZiLoX-IT GbR) (see e.g., Benazzi et al., 2012b; 2013b, c; 2015; 2016; Kullmer et al., 2013; Fiorenza et al., 2015; for more details about methods see SOM).

Metric comparison

Height and breadth of the mandibular corpus at the level of the mental foramen were compared to data gathered from the scientific literature (see SOM Table S1). The BL diameters of the deciduous teeth were compared with a sample of Neandertal, Upper Palaeolithic *H. sapiens* (UPHS) and recent (i.e., post-Neolithic) *H. sapiens* (RHS) teeth collected from the scientific literature (Hillson and Trinkaus, 2002; Henry-Gambier et al., 2004; HersHKovitz et al., 2011). The MD diameter was not considered owing to interproximal wear. For the permanent dentition, comparative datasets for MD and BL diameters were created ex novo and include Neandertal, early (i.e., pre-Upper Palaeolithic) *H. sapiens* (EHS) and RHS (SOM Table S2).

The shape variables (Dzu 1 crown outline; Dzu 2 and SATP5-5 crown and cervical outlines) were projected into the shape-space obtained from a principal component analysis (PCA) of the comparative sample used by Bailey et al. (2014) and Benazzi et al. (2012a), respectively. We used cross-validated linear discriminant analysis (LDA) of the principal components, which accounted for about 90% of the total variability, to assess the taxa most closely affiliated with the Dzu 1, Dzu 2 and SATP5-5 specimens.

Comparative data for 3D enamel thickness were created ex novo and include Neandertal, EHS and RHS with different wear stages (SOM Table S2). The only UPHS specimen available for enamel thickness analysis (Villabruna, lower left first molar; Vercellotti et al., 2008; Oxilia et al. 2015) was included in the RHS sample. To discern differences in enamel thickness between Neandertal and RHS, 3D average enamel thickness (AET) and 3D relative enamel thickness (RET) indices were analyzed using the Mann-Whitney *U* test ($\alpha = 0.05$; two-tailed) with a Monte Carlo

permutation. For sample size > 3 individuals, standardized scores (Z-scores) were computed to establish the group means closest to the values of Dzudzuana and Satsurbliia specimens. The data were processed and analysed using R v. 2.15.1 (R Development Core Team, 2012).

Results

Descriptive data, including provenience, for all the specimens are summarised in Table 1.

Dzudzuana fossils – morphological descriptions

Dzu 1 This specimen is an upper right second deciduous molar (Rdm²), with a complete crown and a cervical quarter of the root (Fig. 1A). The tooth has several visible fractures on the enamel-dentine junction (EDJ; SOM Fig. S2A). While it is heavily worn (wear stage 5; Fig. 1A), the remnants of four principal cusps, a weak Cusp 5 (ASUDAS grade 1), accessory crests and a small Carabelli's trait are still visible on the EDJ (SOM Fig. S2A). The hypocone is small, giving the crown a sub-square shape. Dzu 1 has a distal interproximal facet (length=5 mm; height=1.6 mm) larger than the mesial one (length=3.7 mm; height=1 mm). On the buccal wall of the crown there is a large wear facet with dentine exposure, probably related to para-masticatory activities. Root resorption at the Res3/4 stage suggests that the tooth was lost ante-mortem and corresponds to an age ranging from nine to 12 years old. The tooth crown has a MD diameter of 9.9 mm and a BL diameter of 10.5 mm. At the cervix, the MD diameter is 7.4 mm and BL diameter is 9.9 mm.

Dzu 2 This specimen is a worn (wear stage 4) lower right second deciduous molar (Rdm₂) with a complete crown and a cervical quarter of the root (Fig. 1B). The tooth has several visible fractures, the main one oriented bucco-lingually and dividing the tooth into two parts (see SOM Fig. S4 for the virtual restoration). From the occlusal view, the crown outline shows a bucco-distal reduction and a straighter lingual side (Fig. 1B). On the EDJ, five principal cusps, a weak anterior fovea bordered distally by a weak mesial trigonid crest (MeTC), and potentially the remnant of a distal trigonid crest (DTC), almost entirely removed by tooth wear, can be observed (SOM Fig. S2B).

Interproximal facets are evident both mesially (length=3.7 mm; height=1.7 mm) and distally (length=5.1 mm; height=2.5 mm). Root resorption is at a Res3/4 stage suggesting that the tooth had been lost ante-mortem, at an age ranging from nine to 12 years old. The tooth crown has a MD diameter of 10.3 mm and a BL diameter of 9.5 mm. At the cervix, the MD diameter is 8.6 mm and BL diameter is 7.9 mm.

Figure 1

Testing occlusal contacts between Dzu 1 and Dzu 2

Only three occlusal contacts were detected during maximum intercuspation in the OFA software, ultimately suggesting that the teeth do not belong to the same individual (SOM Fig. S5).

Satsurbilia fossils – morphological descriptions

SATP5-2 This specimen is an upper right central deciduous incisor (Rdi¹), worn (wear stage 4), with the enamel on the mesial side chipped off and the cervical quarter of the root preserved. A longitudinal fracture, bucco-lingually directed, separates a distal portion of the tooth. (Fig. 2). From the labial view, the crown has moderate labial convexity (ASUDAS grade 3), which becomes less pronounced distally. The lingual surface is concave, and shows a distal marginal ridge (the mesial one is not visible, possibly removed by wear) and a faint median ridge, which disappears as it reaches the cervical eminence (Fig. 2). The stage of resorption is at Res1/2 (the preserved portion is 3.5 mm) and suggests that the tooth had been lost ante-mortem through dental development, at an age estimated to be between six and seven years. The tooth crown has a MD diameter of 6.8 mm (minimum estimation due to wear) and a BL diameter of 5.6 mm. At the cervix, the MD diameter is 5.5 mm and BL diameter is 4.9 mm.

Figure 2

SATP5 This specimen is an incomplete left hemi-mandible with part of the body and the ramus preserved (Fig. 3A-C). In detail, the gonial region and the condyle process are missing, as well as the portion of the mandibular body in front of an imaginary line that connects the mental foramen and the alveolus of the left first incisor.

In SATP5, only the second deciduous molar (dm₂; SATP5-5) and the first molar (M₁; SATP5-6) are visible, while premolars (P₃ and P₄, respectively SATP5-3 and SATP5-4) and second molar (M₂; SATP5-7) are unerupted. The teeth, described in more detail below, are well-preserved, except for a small fracture in the P₃. The P₄ is turned upside down, probably from post-depositional repositioning that occurred within the tooth socket. On the lingual side of the hemi-mandible (Fig. 3A), the mylohyoid line runs from the unerupted M₂ till the anterior fracture. On the buccal side (Fig. 3C), the mental foramen is positioned between the interalveolar septa of the deciduous canine and the first deciduous molar. Based on dental development and eruption stages, the age of the individual was estimated to be between six to seven years.

The maximal height of the corpus is 45.7 mm and its maximal length is 69.8 mm. The height of the corpus at the level of the mental foramen is 21.4 mm, with a thickness of 10.5 mm, which is consistent with recent modern humans (see SOM Table S1). At the level of the M₁, the corpus height is 19 mm, with a thickness of 15.5 mm.

Figure 3

SATP5-3 This specimen is a lower left third premolar (LP₃) with a complete, unerupted crown and root in earliest formation, at the R_i developmental stage (Fig. 3G). The crown is sub-circular and shows two main cusps, the protoconid larger than the metaconid, separated by a mesio-distal groove. On the EDJ, two further small dentine horns (hypoconid and entoconid) and a moderate

transverse crest connecting the protoconid and metaconid (grade 2, Bailey, 2002) are visible (SOM Fig. S3A). The tooth crown has a MD diameter of 6.9 mm and a BL diameter of 7.5 mm. At the cervix, the MD diameter is 4.7 mm and BL diameter is 6.5 mm.

SATP5-4 This specimen is a lower left fourth premolar (LP₄) with a complete, unerupted crown but without the root, at the Cr_c developmental stage (Fig. 3H). The crown has a circular occlusal outline and shows four cusps, with the metaconid equal in size to the entoconid (ASUDAS grade 4). The mesio-distal groove separates the main cusps. On the EDJ a mesial accessory ridge (MAR) borders an anterior fovea distally (SOM Fig. S3B). The tooth crown has a MD diameter of 7.2 mm and a BL diameter of 7.9 mm. At the cervix, the MD diameter is 4.5 mm and the BL diameter is 6.4 mm.

SATP5-5 This specimen is a lower left second deciduous molar (Ldm₂) with both crown and root preserved (Fig. 3F). The tooth shows several fractures (see SOM Fig. S3C). While it is very worn (wear stage 4), the five principal cusps forming a Y groove pattern can be recognized, as confirmed by the EDJ. A moderate shoulder on the distal side of the metaconid (SOM Fig. S3C) is identified as C7 (ASUDAS grade 1A). The mesial interproximal wear facets are smaller (length=1.5 mm; height=1.1 mm) than the distal one (length=1.9 mm, height=2.1 mm). On the lingual side, traces of calculus are present (Fig. 3F). The tooth crown has a MD diameter of 10 mm and a BL diameter of 8.7 mm. At the cervix, the MD diameter is 8.3 mm and BL diameter is 7 mm. Root morphology suggests cynodontism, with root bifurcation placed at 2.7 mm from the cervix. The distal root, longer than the mesial one, measures 11.8 mm.

SATP5-6 This specimen is a lower left first molar (LM₁) with crown and root well-preserved (Fig. 3E), at the R1/2 developmental stage. The tooth is slightly worn (category 2), with a weak interproximal facet on the mesial side (length=1.8 mm; height=3.4 mm). In occlusal view, the crown has a rectangular outline and has four main well-developed cusps, an entoconulid (C6) and a faint C7 (ASUDAS grade 1A), also visible on the EDJ (SOM Fig. S3D). The metaconid is in contact with the hypoconid, confirming the classic 4-Y groove pattern. The tooth crown has a MD

diameter of 10.8 mm and a BL diameter of 10.3 mm. At the cervix, the MD diameter is 8.3 mm and the BL diameter is 8.4 mm. The root length measures 9.5 mm on the mesial side, and 8.81 mm on the distal side.

SATP5-7 This specimen is an unerupted lower left second molar (LM₂) with a well-preserved crown and cervical quarter of the root, at the R_i development stage (Fig. 3D). The tooth has four well-developed main cusps arranged in an + pattern, and a faint shoulder identified as a C7 (ASUDAS grade 1A). From this latter develops a weak (grade 1 of Bailey et al., 2011) and continuous DTC (Type 3 following Martínez de Pinillos et al., 2014), visible on the EDJ (SOM Fig. S3E). The tooth crown has a MD diameter of 10.4 mm and a BL diameter of 9.7 mm. At the cervix, the MD diameter is 8.7 mm and the BL diameter is 7.8 mm.

Table 1

Metric comparison

The Z score computed for the BL diameter of Dzu 1 was closer to the UPHS mean, while for Dzu 2 the Z-score was equally close to Neandertals and UPHS. The BL diameter of SATP5-2 was closer to UPHS mean while the BL diameter of SATP5-5 was closer to the RHS mean (Table 2). The permanent teeth of Satsurbliia are small, falling in the range of the whole *H. sapiens* sample (SOM Fig. S6).

Table 2

The Dzu 1 crown outline was projected into the shape-space PCA computed by Bailey and colleagues (2014) and is positioned in PCA space (first two principal components [PCs]) within the recent and UPHS scatter (Fig. 4A, B). The cross-validation LDA of the first four PCs attributes the tooth to modern human with a $P_{\text{post}}=0.99$. Dzu 2 and SATP5-5 crown and cervical

outlines were projected in the shape-space computed by Benazzi and colleagues (2012a). Both outlines of SATP5-5 plots within the whole *H. sapiens* sample (Fig. 4C, D). Whereas, Dzu 2 crown outline falls within *H. sapiens* (Fig. 4C), it falls within Neandertals for the cervical outline due to its bucco-distal enlargement (Fig. 4D). The cross-validated LDA of the first five PCs shows that SATP5-5 is attributed to modern humans with a $P_{\text{post}}=1$, while Dzu2 is attributed to modern humans based on its crown outline ($P_{\text{post}}=1$), but to Neandertals based on its cervical outline ($P_{\text{post}}=0.99$). For the 3D RET of Satsurbliia permanent posterior teeth the Z-scores computed are always closer to the *H. sapiens* mean than to Neandertal ones (Table 3 and SOM Table S3).

Figure 4

Table 3

Discussion and conclusion

Morphological features and morphometric analyses support the attribution of the human remains from Satsurbliia cave and the dm^2 from Dzudzuana cave (Dzu 1) to modern humans. It is possible that because SATP5-2 and SATP5 derive from the same layer and share the same age estimate, they might belong to the same individual. However, this can only be confirmed with further study (i.e. based on ancient DNA). The taxonomic attribution of Dzu 2 is ambiguous, because though the general crown morphology aligns with modern human, the cervical outline plots within Neandertal variation. Moreover, evaluation of the occlusal contacts indicates that Dzu 1 and Dzu 2 do not belong to the same individual. Although it is most likely that Dzu 2 is a modern human specimen, further work is needed (e.g., ancient DNA analysis) to assess the combination of modern human and Neandertal traits. It is important to note, however, that there is no indication in the relevant archaeological contexts to suggest any ‘transitional’ (MP–UP) techno-cultural elements. Even considering the earliest remains uncovered in Dzudzuana, Unit D (dated to

~33,000 cal. BP, see SOM), no attributes of MP cultures are evident. Moreover, the lithic assemblages of Unit C can be considered as a variant of the “Eastern Gravettian” and “Epi-Gravettian” complexes as the lithic industry from the Area B layers, Satsurbliia, from which the human remains described here were recovered (Bar-Yosef et al., 2011; Pinhasi et al. 2014).

Our current study demonstrates the potential of the OFA software for associating isolated teeth. In a previous contribution, two isolated teeth from Taddeo Cave (Italy) were attributed to the same individual by matching the interproximal facets in the OFA software (Benazzi et al., 2011c). The approach is extended here to use the OFA software in matching isolated antagonistic teeth, which follows recent work that suggests close correspondence in macrowear pattern between antagonists (Kullmer et al., 2012). In the current study, we also provide new data on the 3D enamel thickness of Neandertal and modern human lower molars and premolars at different wear stages following recent protocols (Benazzi et al., 2014b) taking into consideration the current lack of comparative data for both lower and upper premolars. Our results confirm that Neandertal M₂s have significantly lower RET indices than those of modern humans (Olejniczak et al., 2008; Smith et al., 2012). However, contrary to our expectations and previous contributions (Macchiarelli et al., 2006; Olejniczak et al., 2008; Bayle et al., 2010; Smith et al., 2012), there is no statistically significant difference between the M₁s of the two groups, so our results indicate that they cannot be discriminated securely. Nonetheless, differences between the two groups appear pronounced in the premolars, suggesting that P₃s and P₄s may be valuable in discriminating between Neandertals and modern humans. Interestingly, even though the small sample size prevents statistical tests, differences seem to persist at least in wear stage 3, rendering the lower post-canine dentition, and particularly the premolars, useful discriminatory tooth classes even when affected by moderate dental wear.

In sum, the analyses of the modern human remains from Dzudzuana and Satsurblia caves provide a major addition to the UP human fossil record of Georgia and indicate the unequivocal presence of modern humans in Georgia during the Upper Palaeolithic, undermining the suggestion that Caucasus represents a cul de sac for Neandertal survival (Bar-Yosef and Pilbeam 2000). Even though this region is characterized by several Palaeolithic sites, only two other cave sites (Bondi Cave and Sakajia) have yielded human remains from UP deposits. It is important to note that the chronological age of the teeth from Dzudzuana cave (27,000–24,000 cal. BP) falls between the older modern human tooth Bondi I (Pleurdeau et al., 2016) and the more recent human remains from Sakajia (Nioradze and Otte, 2000), filling the huge gap of more than 20,000 years.

Acknowledgements

The authors are grateful to Heiko Temming for technical support for the metric comparison sample provided by the Department of Human Evolution, Max Planck Institute for Evolutionary Anthropology (Leipzig). We also thank Tommaso Saccone for the elaboration of the general map that showing the location of Dzudzuana, Satsurblia caves and the other Georgian sites. Finally, thanks to Rosa Conte for proofreading this manuscript. This project has received funding from the European Research Council (ERC) under the European Union's Horizon 2020 research and innovation programme (grant agreement No 724046 - SUCCESS); www.erc-success.eu

References

- AlQahtani, S.J., Hector, M.P., Liversidge, H.M., 2010. Brief communication: The London atlas of human tooth development and eruption. *Am. J. Phys. Anthropol.* 142, 481–490.
- Bailey, S.E., 2002. A closer look at Neanderthal postcanine dental morphology: the mandibular dentition. *Anat. Rec* 269, 148–156.
- Bailey, S.E., Skinner, M.M., Hublin, J.J., 2011. What lies beneath? An evaluation of lower molar trigonid crest patterns based on both dentine and enamel expression. *Am. J. Phys. Anthropol.* 145, 505–518.
- Bailey, S.E., Benazzi, S., Souday, C., Astorino, C., Paul, K., Hublin, J.J., 2014. Taxonomic differences in deciduous upper second molar crown outlines of *Homo sapiens*, *Homo neanderthalensis* and *Homo erectus*. *J. Hum. Evol.* 72, 1–9.
- Bar-Yosef, O., Pilbeam D., (Ed.), 2000. The Geography of Neandertals and Modern Humans in Europe and the Greater Mediterranean. Volume Bulletin No. 8. Peabody Museum Press, Harvard University, Cambridge. Check it's really Volume Bulletin
- Bar-Yosef, O., Belfer-Cohen, A., Mesheviliani, T., Jakeli, N., Bar-Oz, G., Boaretto, E., Goldberg, P., Kvavadze, E., Matskevich, Z., 2011. Dzudzuana: an Upper Palaeolithic cave site in the Caucasus foothills (Georgia). *Antiquity* 85, 331–349.
- Bayle, P., Macchiarelli, R., Trinkaus, E., Duarte, C., Mazurieri, A., Zilhão, J., 2010. Dental maturational sequence and dental tissue proportions in the early Upper Paleolithic child from

Abrigo do Lagar Velho, Portugal. PNAS 107, 1338-1342.

Benazzi, S., Coquerelle, M., Fiorenza, L., Bookstein, F., Katina, S., Kullmer, O., 2011a. Comparison of dental measurement systems for taxonomic assignment of first molars. *Am. J. Phys. Anthropol.* 144, 342-354.

Benazzi, S., Douka, K., Fornai, C., Bauer, C.C., Kullmer, O., Svoboda, J.J., Pap, I.I., Mallegni, F., Bayle, P., Coquerelle, M., Condemi, S., Ronchitelli, A., Harvati, K., Weber, G.W., 2011b. Early dispersal of modern humans in Europe and implications for Neanderthal behaviour. *Nature* 479, 525-528.

Benazzi, S., Viola, B., Kullmer, O., Fiorenza, L., Harvati, K., Paul, T., Gruppioni, G., Weber, G.W., Mallegni, F., 2011c. A reassessment of the Neanderthal teeth from Taddeo cave (southern Italy). *J. Hum. Evol.* 61, 377-387.

Benazzi, S., Fornai, C., Buti, L., Toussaint, M., Mallegni, F., Ricci, S., Gruppioni, G., Weber, G.W., Condemi, S., Ronchitelli, A., 2012a. Cervical and crown outline analysis of worn Neanderthal and modern human lower second deciduous molars. *Am. J. Phys. Anthropol.* 149, 537-546.

Benazzi, S., Kullmer, O., Grosse, I., Weber, G., 2012b. Brief communication: comparing loading scenarios in lower first molar supporting bone structure using 3D finite element analysis. *Am. J. Phys. Anthropol.* 147, 128-134.

Benazzi, S., Bailey, S.E., Mallegni, F., 2013a. Brief communication: A morphometric analysis of the Neandertal upper second molar Leuca I. *Am. J. Phys. Anthropol.* 152, 300-305.

Benazzi, S., Nguyen, H.N., Schulz, D., Grosse, I.R., Gruppioni, G., Hublin, J.J., Kullmer, O., 2013b. The evolutionary paradox of tooth wear: simply destruction or inevitable adaptation? PLOS ONE 8, e62263.

Benazzi, S., Nguyen, H.N., Kullmer, O., Hublin, J.J., 2013c. Unravelling the functional biomechanics of dental features and tooth wear. PLOS ONE 8, e69990.

Benazzi, S., Bailey, S.E., Peresani, M., Mannino, M.A., Romandini, M., Richards, M.P., Hublin, J.J., 2014a. Middle Paleolithic and Uluzzian human remains from Fumane cave, Italy. J. Hum. Evol. 70, 61-68.

Benazzi, S., Panetta, D., Fornai, C., Toussaint, M., Gruppioni, G., Hublin, J.J., 2014b. Technical Note: Guidelines for the digital computation of 2D and 3D enamel thickness in hominoid teeth. Am. J. Phys. Anthropol. 153, 305-313.

Benazzi, S., Nguyen, H.N., Kullmer, O., Hublin, J.J., 2015. Exploring the biomechanics of taurodontism. J. Anat. 226, 180-8.

Benazzi, S., Nguyen, H.N., Kullmer, O., Kupczik, K., 2016. Dynamic modelling of tooth deformation using occlusal kinematics and finite element analysis. PLOS ONE 11, e0152663.

Buikstra, J.E., Ubelaker, D.H. (Eds.), 1994. Standards for data collection from human skeletal remains: proceedings of a seminar at the Field Museum of Natural History. Arkansas Archeological Survey Research Series No. 44.

Fiorenza, L., Nguyen, H.N., Benazzi, S., 2015. Stress distribution and molar macrowear in *Pongo pygmaeus*: a new approach through finite element and occlusal fingerprint analyses. Hum. Evol. 30, 215-226.

Henry-Gambier, D., Maureille, B., White, R., 2004. Vestiges Humains Des Niveaux De L ' Aurignacien Ancien Du Site De Brassempouy (Landes). Bulletins et mémoires de la Société d'Anthropologie de Paris 16, 49-87. The title should probably be lower case - please check

Hershkovitz, I., Smith, P., Sarig, R., Quam, R., Rodríguez, L., García, R., Arsuaga, J.L., Barkai, R., Gopher, A., 2011. Middle Pleistocene dental remains from Qesem Cave (Israel). Am. J. Phys. Anthropol. 144, 575-592.

Hillson, S.W., Trinkaus, E., 2002. Comparative dental crown metrics. In: Zilhão, J., Trinkaus, E. (Eds.), Portrait of the Artist as a Child. The Gravettian Human Skeleton from the Abrigo do Lagar Velho and its Archeological Context. Trabalhos de Arqueologia Vol. 22, Instituto Português de Arqueologia, Lisboa, pp. 356-364.

Kullmer, O., Schulz, D., Benazzi, S., 2012. An experimental approach to evaluate the correspondence between wear facet position and occlusal movements. Anat. Rec. 295, 846-852.

Kullmer, O., Benazzi, S., Schulz, D., Gunz, P., Kordos, L., Begun, D.R., 2013. Dental arch restoration using tooth macrowear patterns with application to *Rudapithecus hungaricus*, from the late Miocene of Rudabánya, Hungary. J. Hum. Evol. 64, 151-160.

Macchiarelli, R., Bondioli, L., Debenath, A., Mazurier, A., Tournepiche, J.F., Birch, W., Dean, M.C., 2006. How Neanderthal molar teeth grew. Nature 444, 748-751.

- Margherita, C., Talamo, S., Wiltchke-Schrotta, K., Senck, S., Oxilia, G., Sorrentino, R., Mancuso, G., Gruppioni, G., Lindner, R., Hublin, J.J., Benazzi, S., 2016. A reassessment of the presumed Torrener Bärenhöhle's Paleolithic human tooth. *J. Hum. Evol.* 93, 120-125.
- Martínez de Pinillos, M., Martínón-Torres, M., Skinner, M.M., Arsuaga, J.L., Gracia-Téllez, A., Martínez, I., Martín-Francés, L., Bermúdez de Castro, J.M., 2014. Trigonid crests expression in Atapuerca-Sima de los Huesos lower molars: Internal and external morphological expression and evolutionary inferences. *C.R. Palevol* 13, 205-221.
- Molnar, S., 1971. Human tooth wear, tooth function and cultural variability. *Am. J. Phys. Anthropol.* 34, 175-189.
- Moorrees, C.F.A., 1963. Formation and resorption of three deciduous teeth in children. *Am. J. Phys. Anthropol.* 21, 205-213.
- Nioradze, M.G., Otte, M., 2000. Paleolithique superieur de Georgie. *Anthropologie* 104, 265-300.
- Olejniczak, A.J., Smith, T.M., Feeney, R.N.M., Macchiarelli, R., Mazurier, A., Bondioli, L., Rosas, A., Fortea, J., de la Rasilla, M., Garcia-Tabernero, A., Radovčić, J., Skinner, M.M., Toussaint, M., Hublin, J.J., 2008. Dental tissue proportions and enamel thickness in Neandertal and modern human molars. *J. Hum. Evol.* 55, 12-23.
- Oxilia, G., Peresani, M., Romandini, M., Matteucci, C., Debono Spiteri, C., Henry, A.G., Schulz, D., Archer, W., Crezzini, J., Boschin, F., Boscato, P., Jaouen, K., Dogandzic, T., Broglio, A., Moggi-Cecchi, J., Fiorenza, L., Hublin, J.J., Kullmer, O., Benazzi, S., 2015. Earliest evidence of

dental caries manipulation in the Late Upper Palaeolithic. *Sci. Rep.* 5, 12150.

Panetta, D., Belcari, N., Del Guerra, A., Bartolomei, A., Salvadori, P.A., 2012. Analysis of image sharpness reproducibility on a novel engineered micro-CT scanner with variable geometry and embedded recalibration software. *Phys. Medica* 28, 166-173.

Pinhasi, R., Nioradze, M., Tushabramishvili, N., Lordkipanidze, D., Pleurdeau, D., Moncel, M.-H., Adler, D.S., Stringer, C., Higham, T.F.G., 2012. New chronology for the Middle Palaeolithic of the southern Caucasus suggests early demise of Neanderthals in this region. *J. Hum. Evol.* 63, 770-780.

Pinhasi, R., Meshveliani, T., Matskevich, Z., Bar-Oz, G., Weissbrod, L., Miller, C.E., Wilkinson, K., Lordkipanidze, D., Jakeli, N., Kvavadze, E., Higham, T.F.G., Belfer-Cohen, A., 2014. Satsurblia: New insights of human response and survival across the last glacial maximum in the southern caucasus. *PLOS ONE* 9, e111271.

Pleurdeau, D., Moncel, M.-H., Pinhasi, R., Yeshurun, R., Higham, T., Agapishvili, T., Bokeria, M., Muskhelishvili, A., Le Bourdonnec, F.-X., Nomade, S., Poupeau, G., Bocherens, H., Frouin, M., Genty, D., Pierre, M., Pons-Branchu, E., Lordkipanidze, D., Tushabramishvili, N., 2016. Bondi Cave and the Middle-Upper Palaeolithic transition in western Georgia (south Caucasus). *Quaternary Sci. Rev.* 146, 77-98.

Rosas, A., Bermúdez de Castro, J.M., 1999. The ATD6-5 mandibular specimen from Gran Dolina (Atapuerca, Spain). Morphological study and phylogenetic implications. *J. Hum. Evol.* 37, 567-590.

Scott, R.G., Turner, C.I., 1997. The Anthropology of Modern Human Teeth: Dental Morphology and its Variation in Recent Human Population. Cambridge University Press, Cambridge.

Smith, T.M., Olejniczak, A.J., Zermeno, J.P., Tafforeau, P., Skinner, M.M., Hoffmann, A., Radovic, J., Toussaint, M., Kruszynski, R., Menter, C., Moggi-Cecchi, J., Glasmacher, U.A., Kullmer, O., Schrenk, F., Stringer, C., Hublin, J.J., 2012. Variation in enamel thickness within the genus *Homo*. *J. Hum. Evol.* 62, 395-411.

Turner II, C.G., Nichol, C.R., Scott, G.R., 1991. Scoring procedures for key morphological traits of the permanent dentition: The Arizona State University Dental Anthropology System. In: Kelley, M.A., Larsen, C.S. (Eds.), *Advances in Dental Anthropology*. Wiley-Liss, New York, pp. 13-31.

Tushabramishvili, N., Pleurdeau, D., Moncel, M.H., Agapishvili, T., Vekua, A., Bukhsianidze, M., Maureille, B., Muskhelishvili, A., Mshvildadze, M., Kapanadze, N., Lordkipanidze, D., 2012. Human remains from a new Upper Pleistocene sequence in Bondi Cave (Western Georgia). *J. Hum. Evol.* 62, 179-185.

Vercellotti, G., Alciati, G., Richards, M., Formicola, V., 2008. The Late Upper Paleolithic skeleton Villabruna 1 (Italy): A source of data on biology and behavior of a 14.000 year-old hunter. *J. Anthropol Sci.* 86, 143–163.

White, T.D., Black, M.T., Folkens, P.A., (Ed.), 2012. *Human Osteology*, Third. ed. Elsevier. London.

Table 1

Inventory of the human remains from Dzudzuana (Dzu) and Satsurbliia (SATP5) caves.

Specimen	Tooth class	MD	BL	Wear stage^a	Estimated age (years)^{b,c}	Stratigraphic Unit	Culture
Dzu 1	Rdm ²	9.9	10.5	5	9-12	Layer C3	Upper Palaeolithic
Dzu 2	Rdm ₂	10.3	9.5	4	9-12	Layer C4	Upper Palaeolithic
SATP5-2	Rdi ¹	6.8	5.6	4	6-7	Area B	Upper Palaeolithic
Mandible SATP5					6-7	Area B	Upper Palaeolithic
SATP5-3	LP ₃	6.9	7.5	1			
SATP5-4	LP ₄	7.2	7.9	1			
SATP5-5	Ldm ₂	10.0	8.7	4			
SATP5-6	LM ₁	10.8	10.3	2			
SATP5-7	LM ₂	10.4	9.7	1			

^a Molnar, 1971.^b Moorrees, 1963.^c Al Qahtani et al., 2010.

Table 2

Buccolingual (BL) diameters (in mm) of the comparative sample and Z-scores of the deciduous teeth from Dzudzuana and Satsurblia standardized to the hominin samples used in this study (N, Neandertal; UPHS, Upper Palaeolithic *H. sapiens*; RHS, recent *H. sapiens*; SD, standard deviation).

Sample	Dzu 1		Dzu 2		SATP5-2		SATP5-5	
	(Rdm ²)		(Rdm ₂)		(Rdi ¹)		(Ldm ₂)	
	Mean (SD/n)	Z-score	Mean (SD/n)	Z-score	Mean (SD/n)	Z-score	Mean (SD/n)	Z-score
N	10.2 (0.7/13) ^a	0.48	9.4 (0.5/34) ^b	0.26	6.13 (0.35/23) ^b	-1.45	9.4 (0.5/34) ^b	-1.4
UPHS	10.4 (0.7/11) ^a	0.2	9.44 (0.35/8) ^c	0.26	5.42 (0.35/18) ^b	0.57	9.44 (0.35/8) ^c	-2.11
RHS	9.5 (0.5) ^a	2.08	8.3 (0.6/57) ^b	2.05	4.87 (0.35/47) ^b	2.14	8.3 (0.6/57) ^b	0.67

^a Hillson and Trinkaus, 2002.

^b Hershkovitz et al., 2011.

^c Henry-Gambier et al., 2004.

Table 3Three-dimensional (3D) relative enamel thickness (RET).^a

Sample	<i>n</i>	Wear ^b	3D RET Mean (SD)	Z-score
SATP5-3 (LP₃)		1	26.75	
N	8	1-2	18.55 (1.60)	5.12
RHS	11	1-2	24.39 (2.38)	0.99
RHS	4	3	19.60 (0.93)	7.69
SATP5-4 (LP₄)		1	41.46	
N	11	1-2	20.62 (2.37)	8.79
RHS	8	1-2	25.69 (2.22)	7.10
RHS	4	3	25.01 (4.46)	3.69
SATP5-6 (LM₁)		2	20.47	
N	8	1-2	18,61 (1.59)	1.17
N	6	3	15,86 (1.33)	3.47
N	9	4	12,21 (1.66)	4.97
RHS	8	1-2	20.17 (3.50)	0.29
RHS	8	3	16.16 (1.98)	2.18
RHS	5	4	14.30 (2.34)	2.64
SATP5-7 (LM₂)		1	23.7	
N	9	1-2	17.42 (2.60)	2.41
RHS	9	1-2	21.61 (1.73)	1.20

^aSatsurblia specimens are standardized to Z-scores of the Neandertal (N) and recent *H. sapiens* (RHS) samples for different wear stages. SD = standard deviation.

^bMolnar, 1971.

Figure legends

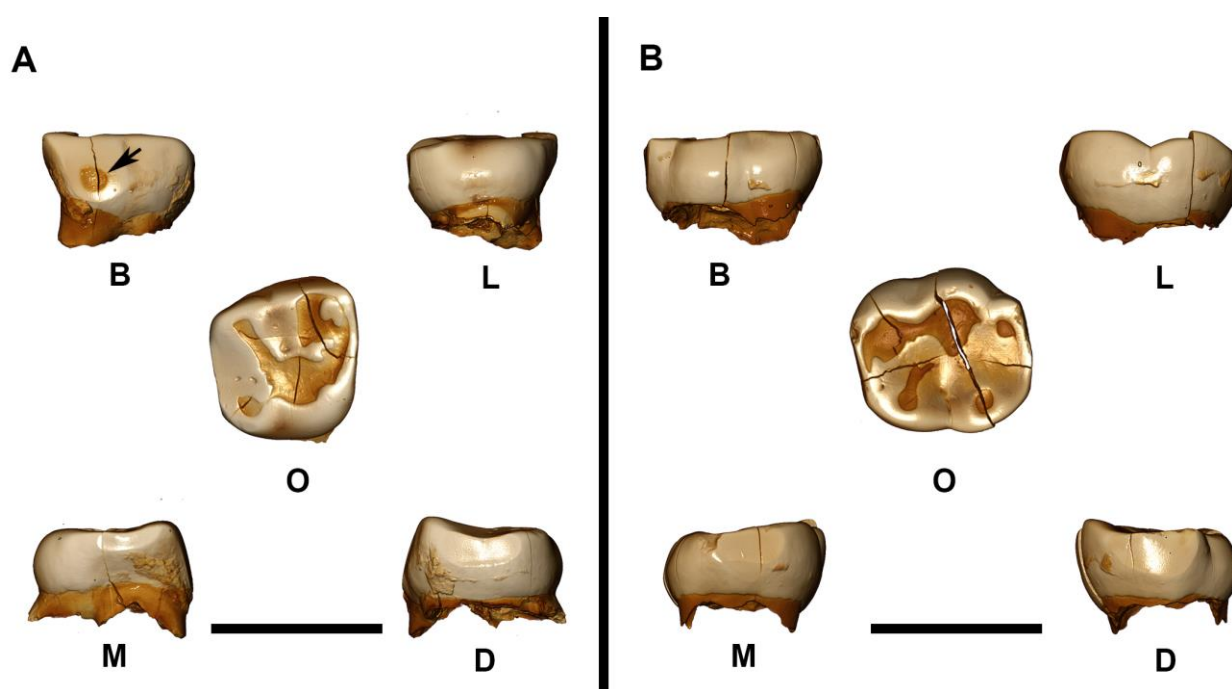


Figure 1. A) Three-dimensional digital models of Dzu 1 (upper right second deciduous molar, Rdm2); B) Three-dimensional digital model of Dzu 2 (lower right second deciduous molar, Rdm2). The horizontal black bars are equivalent to 1 cm. B, buccal; D, distal; L, lingual; M, mesial; O, occlusal.

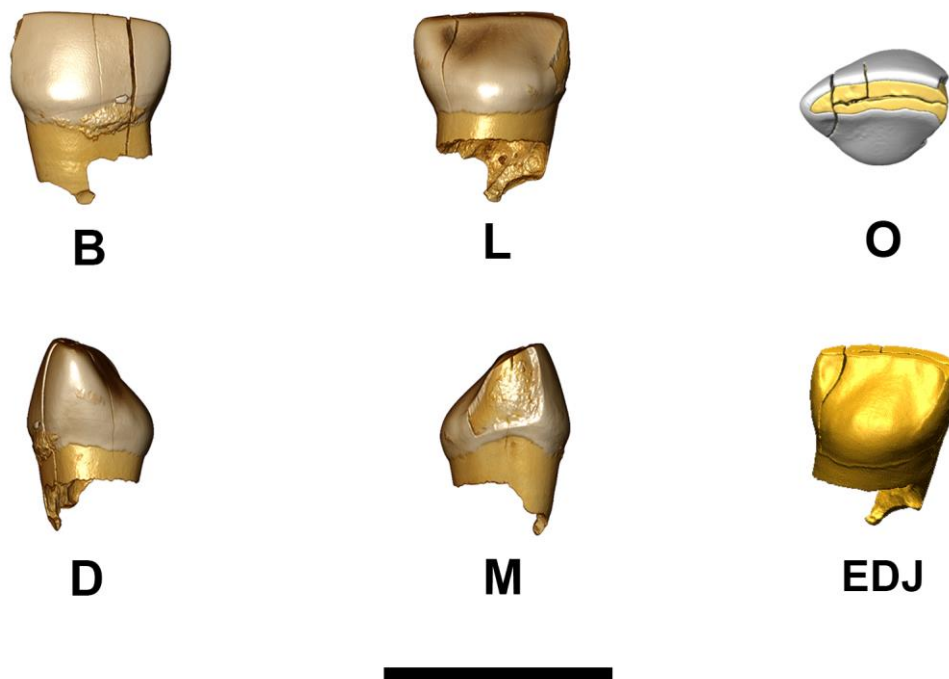


Figure 2. Three-dimensional digital model of SATP5-2 (upper right central deciduous incisor, Rdi1). The horizontal black bar is equivalent to 1 cm. B, buccal; D, distal; L, lingual; M, mesial; O, occlusal; EDJ, enamel-dentine junction.

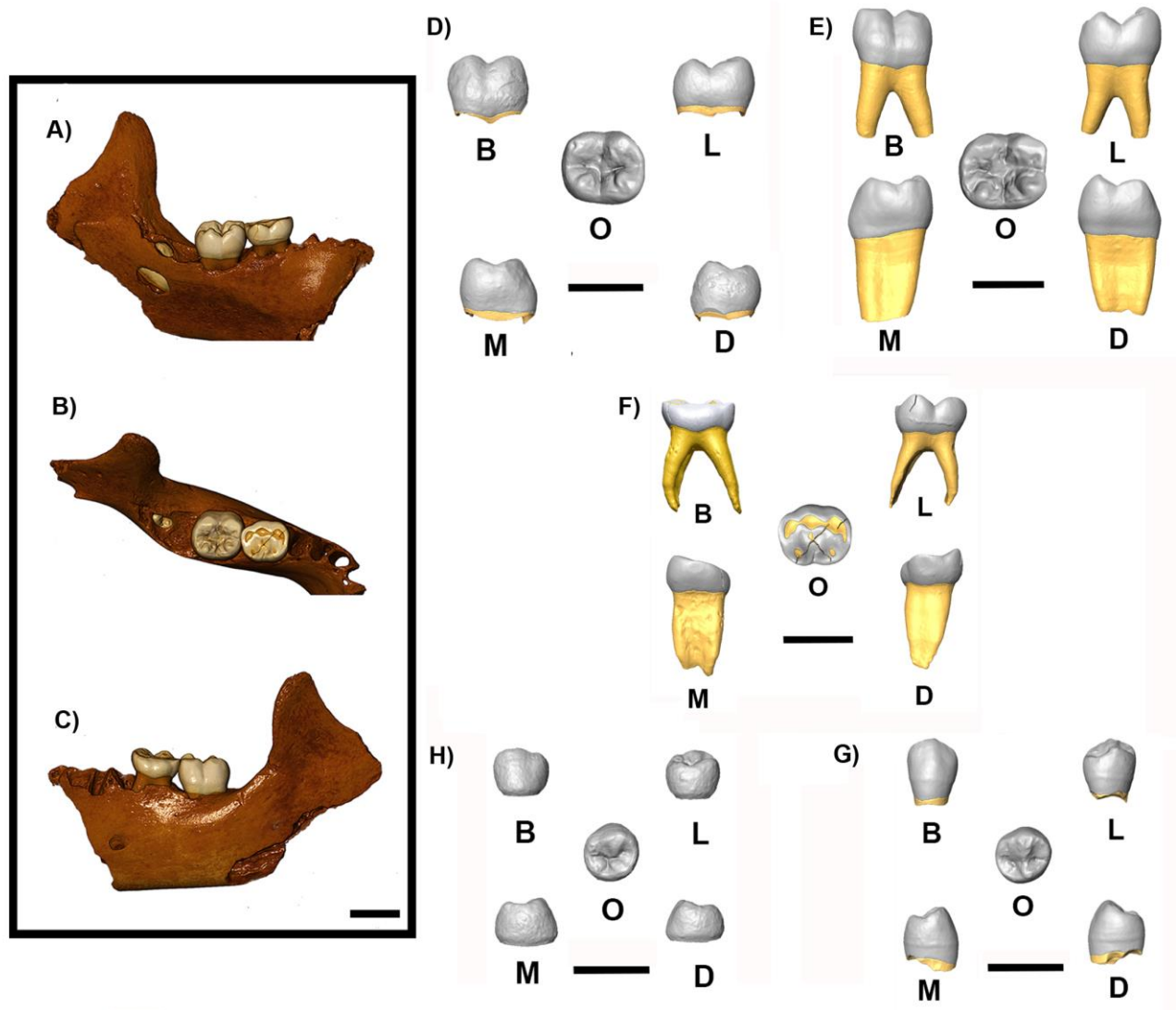


Figure 3. On the left, three-dimensional digital model of Satsurbliia mandible (SATP5): A) Lingual side; B) Occlusal side; C) Buccal side. On the right, three-dimensional digital models of: D) SATP5-7 (lower left second molar, LM2); E) SATP5-6 (lower left first molar, LM1); F) SATP5-5 (left second deciduous molar, Ldm2); G) SATP5-3 (lower left third premolar, LP3); H) SATP5-4 (lower left fourth premolar, LP4). The horizontal black bars are equivalent to 1 cm. B, buccal; D, distal; L, lingual; M, mesial; O, occlusal.

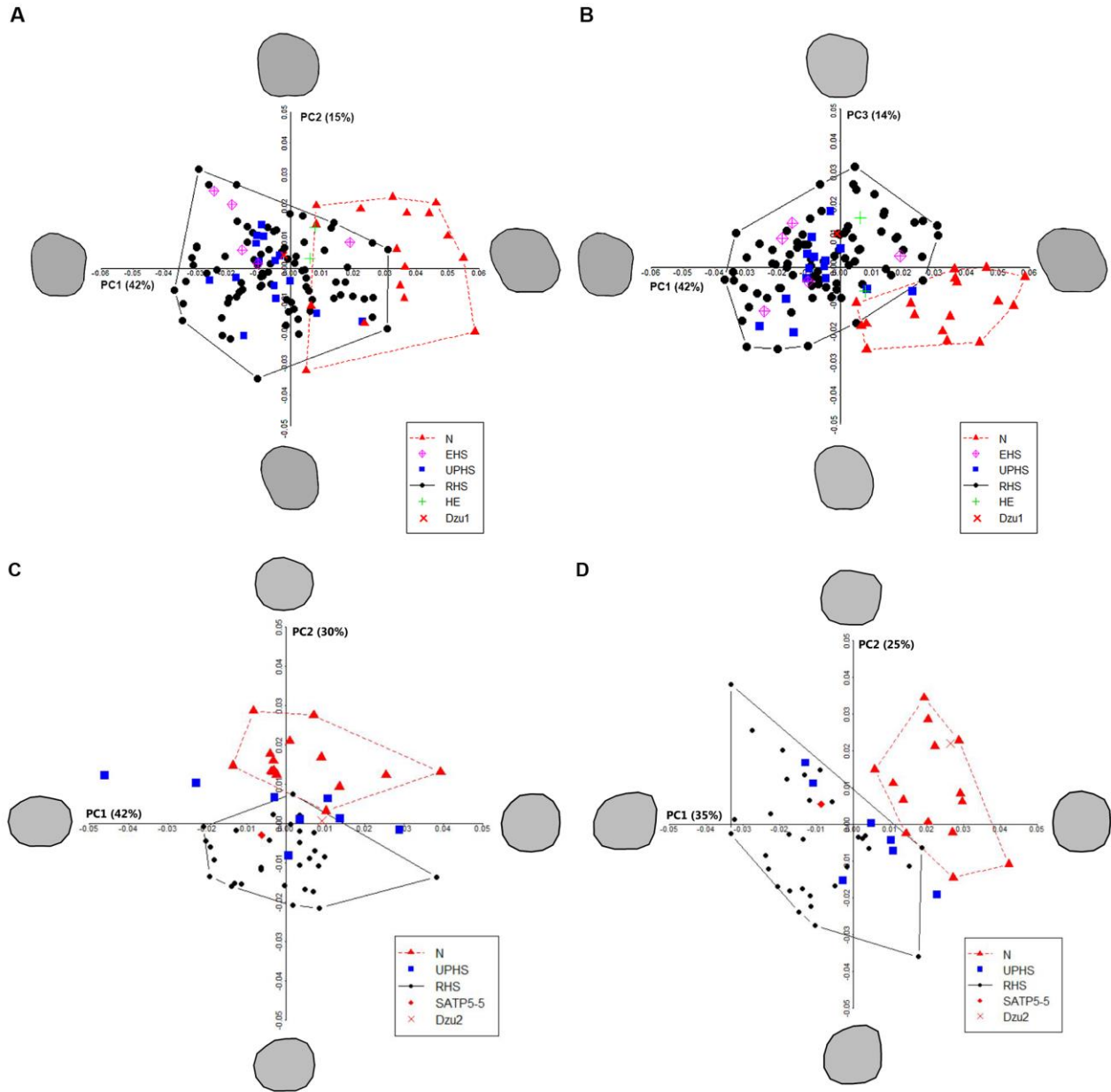


Figure 4. A, B) Shape-space PCA plots of *Homo erectus*, Neandertal and *H. sapiens* (EHS; UPHS; RHS) dms2 crown outlines. A) PC1 plotted against PC2; B) PC1 plotted against PC3. The deformed mean outlines in the four directions of the PCs are drawn at the extremity of each axis. C, D) Shape-space PCA plots of Neandertal and *H. sapiens* (RHS and UPHS) dm2 crown outlines (C), and cervical outlines (D). The deformed mean outlines in the four directions of the PCs are drawn at the extremity of each axis. HE, *H. erectus*; N, Neandertal; EHS, early *H. sapiens*; UPHS, Upper Palaeolithic *H. sapiens*; RHS, recent *H. sapiens*.

Supplementary Online Material (SOM)

Index

1. Archaeological contexts

1.1 Dzudzuana cave

1.2 Satsurbliia cave

2. Materials and methods

2.1 Micro-CT

2.2 Morphometric analyses

3. Results

3.1 Testing occlusal contacts between Dzu 1 and Dzu 2

3.2 Mandible

3.3 Metric comparison

4. References

5. Tables

6. Legend for supporting illustrations

1. Archaeological contexts

1.1 *Dzudzuana cave*

The cave of Dzudzuana (Western Georgia [Fig. S1]) was the first to provide a well-dated Upper Palaeolithic (UP) chronostratigraphic sequence for human occupation in the southern Caucasus (Bar-Yosef et al., 2011, their Fig. 2). This sequence comprises three occupational episodes separated by millennia long hiatuses: the lowermost UP phase, Unit D, is dated to 34,500–32,200 calendar years (cal. BP [calibrated years before present]); the following Unit C, is dated to 27,000–24,000 cal. BP (the human teeth studied were retrieved from the lower part of this Unit, in a distinct anthropogenic layer, mixed with chipped stone artefacts and fauna remains); and the latest UP phase, Unit B - dated to 16,500–13,200 cal. BP (Bar-Yosef et al., 2011, their Fig. 3).



Figure S1. Georgia - A general map showing the location of Dzudzuana, Satsurblia caves and the other sites mentioned in the paper (Google Earth).

The chipped stone assemblage of Unit C (which comprises the main material culture remains) is dominated by small blades and bladelets detached predominantly from narrow carinated cores. Besides retouched bladelets, there are the Sakajia points (arched/curved pointed blades with abrupt retouch along the straight edge and a proximal retouched truncation). It is of interest to note the decorative items recovered in this Unit. There were pendants made of stone, bone and teeth (of goats and deer) (Bar-Yosef et al., 2011, their Fig. 6). Other decorated items include incised bone pieces, sometimes with elaborate patterns, of either long bone splinters or ribs. Quite a number of bone tools (and see detailed discussion in Bar-Yosef et al., 2011) were recovered, mostly awls/points made on splinters, shaped by shaving and polishing. Besides those there were also decorated items, polishers, and a single bone needle with an ‘eye’, according well with the findings in all UP Units of wild flax fibers (Kvavadze et al., 2009).

1.2 Satsurbliā cave

The human occupation layers at Satsurbliā cave yielded a series of living surfaces dated to (a) prior to the Last Glacial Maximum (LGM) at 25,500–24,400 cal. BP and (b) after the LGM at 17,900–16,200 cal. BP. Excavations were conducted in two main areas: Area A and Area B (Pinhasi et al., 2014, Fig. 2).

Area A is situated in the northwestern part of the cave, near the entrance and Area B is in the rear of the cave adjacent to a trench excavated in the early 1990s. Both areas revealed stratigraphic sequences comprising Pleistocene (UP) and Holocene (Eneolithic and later) deposits. In both areas, the in situ UP layers were extremely rich in anthropogenic remains (e.g., a circular fireplace, large quantities of charcoal and burnt bones, lithics, bone tools, shell ornaments, yellow ochre). The UP sequence of Area A was divided into two main units: A/I and A/II. A/II contained a sequence of living surfaces which were dated (surface II and III) to 17,000–18,000 cal. BP and as such are the first well-dated evidence for human occupation in the southern Caucasus at the end

of the LGM. This fills in a gap in the local UP sequence, namely that between Unit C and Unit B in Dzudzuana cave (western Georgia), dated to 27,000–24,000 cal. BP and 16,000 cal. BP – 13,200 cal. BP, respectively (Pinhasi et al., 2014, Fig. 3). The stratigraphic sequence of Area B includes so far four main archaeological layers (B/I, B/II, B/III, B/IV) and reaches a thickness of >2 m (6.5 m below the datum). Layer B/III is dated to 25,220–24,440 cal. BP (with dates pending for the underlying layer B/IV) (Pinhasi et al., 2014, their Fig. 6). An isolated tooth (SATP5-2) and a hemi-mandible (SATP5) with teeth (LP₃ = SATP5-3, LP₄ = SATP5-4, Ldm₂ = SATP5-5, LM₁ = SATP5-6, LM₂ = SATP5-7) have been recovered from a poorly provenienced UP context in Area B (excavated in the 1990s). The hemi-mandible was directly dated to 11,250 ± 50 BP (OxA-26862) (the specimen was analyzed at Oxford Radiocarbon Laboratory for AMS 14C dating). The obtained radiometric date provides a calibrated range of 13,031-13,225 cal. BP, using Oxcal 4.2 with IntCal 13 calibration curve. The specimen was well preserved, and yielded 13.32% collagen by weight (in modern unadulterated bone, ~20% by weight is collagen) and the C:N atomic ratio was 3.2 (in modern bone, this measure is around 3.21). Its direct date indicates that it is from the late UP occupation phase in Satsurblia. In general, the UP lithic assemblages in Satsurblia differ from those of Dzudzuana Unit C. Though they also represent mostly a bladelet industry, the dominant tool types are obliquely truncated retouched/backed bladelets with some microgravettes and rare Gravette points (Pinhasi et al., 2014).

2. Materials and methods

2.1 Micro-CT

High-resolution micro-CT images of the teeth from Dzudzuana (Dzu 1 and Dzu 2; main text Fig. 1) and the isolated tooth from Satsurblia (SATP5-2) (Fig. 2) were obtained with a XALT microtomographic system (Institute of Clinical Physiology, Pisa, Italy) (Panetta et al., 2012) using the following scan parameters: 50 kV, 0.7 mA, with a 2mm Aluminium filter. The Satsurblia mandible (Fig. 3) was scanned with a Birscan microtomographic system (Max Planck Institute for Evolutionary Anthropology, Leipzig, Germany) using the following scan parameters: 130 kV, 0.1

mA, with a 0.50 mm Brass filter. Volume data were reconstructed using isometric voxels of 18.4 μm for the isolated teeth and 30.15 μm for the mandible.

The image stacks were segmented with a semiautomatic approach in Avizo 7.0 (Visualization Sciences Group Inc.) in order to separate the tissues and to reconstruct three-dimensional (3D) digital models of the teeth and of the mandible, which were then used to support the morphological description and to collect morphometric data (SOM Fig. S2, S3).

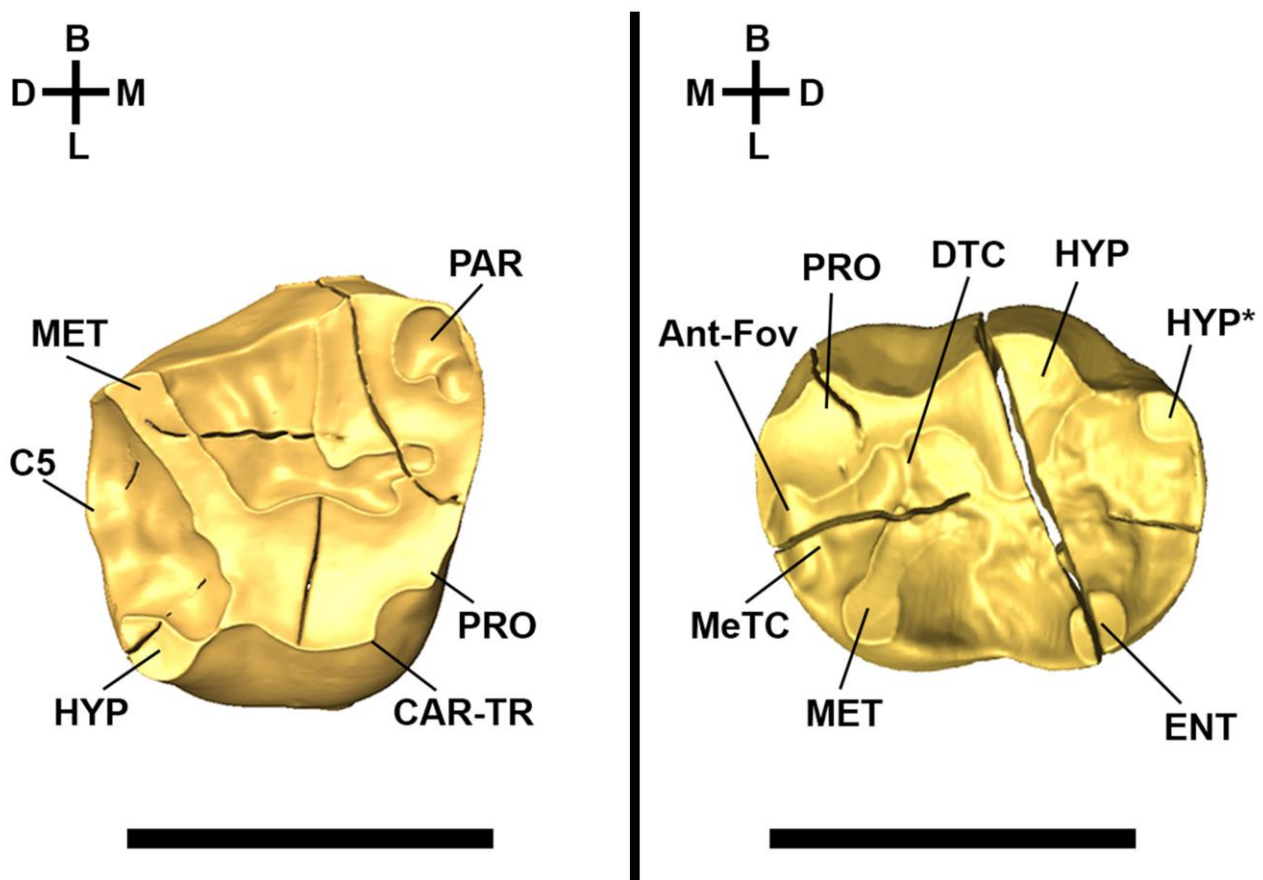


Figure S2. A) Three-dimensional digital models of the enamel-dentine junction (EDJ) of Dzu 1.

PRO = protocone; PAR = paracone; MET = metacone; HYP = hypocone; C5 = fifth cusp; CAR-

TR = Carabelli's trait. B) Three-dimensional digital model of the EDJ of Dzu 2. PRO =

protoconid; MET = metaconid; HYP = hypoconid; HYP* = hypoconulid; ENT = Entoconid;

MeTC = mesial trigonid crest; DTC = distal trigonid crest; Ant-Fov = anterior fovea. The black

bar is equivalent to 1 cm. B, buccal; D, distal; L, lingual; M, mesial; O, occlusal.

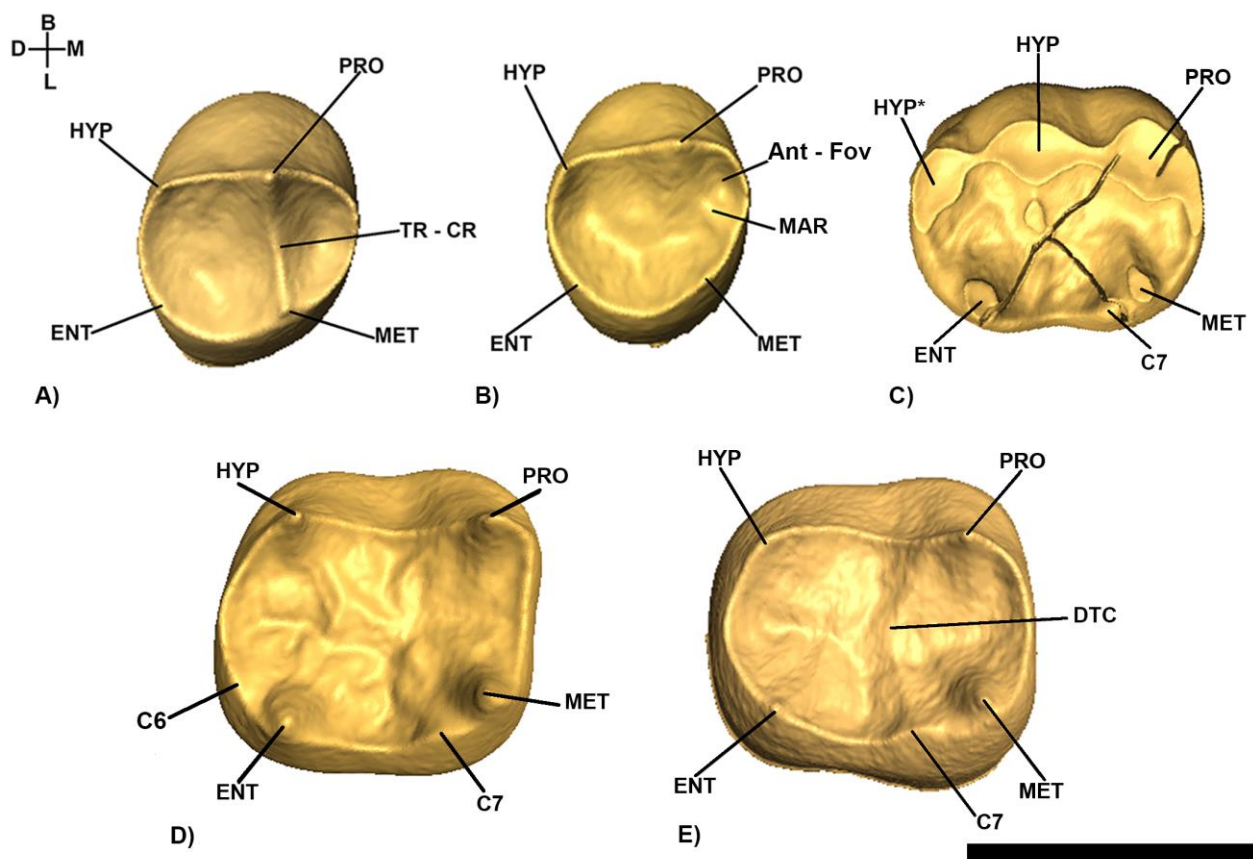


Figure S3. A) Three-dimensional digital models of the EDJ of: A) SATP5-3 (lower left third premolar, LP₃), B) SATP5-4 (lower left fourth premolar, LP₄), C) SATP5-5 (left second deciduous molar, Ldm₂), D) SATP5-6 (lower left first molar, LM₁), E) SATP5-7 (lower left second molar, LM₂). PRO = protoconid; MET = metaconid; HYP = hypoconid; ENT = entoconid; HYP* = hypoconulid; C6 = sixth cusp or entoconulid; C7 = seventh cusp or metoconulid; TR – CR = transverse crest; MAR = mesial accesory ridge; Ant-Fov = anterior fovea; DTC = distal trigonid crest. The black bar is equivalent to 1 cm. B, buccal; D, distal; L, lingual; M, mesial; O, occlusal.

2.2 Morphometric analyses

Height of the mandibular corpus was measured perpendicular to the alveolar plane, and its breadth was taken at the maximum width of the mandibular corpus (Buikstra and Ubelaker, 1994; Rosas and Bermúdez de Castro, 1999).

The digital models of all the teeth, including the comparison sample, were optimized (e.g., healing defects) and oriented in Rapidform XOR2 (INUS Technology, Inc., Seoul, Korea) before the morphometric analyses. For Dzu 2, a virtual restoration was required before the analyses. This was carried out by moving the distal portion of the tooth until continuity in the cervical line, occlusal and lateral surface of the crown was restored (SOM Fig. S4). Each tooth was oriented by aligning the cervical plane (computed as the best-fit plane at the cervical line) parallel to the xy-plane of the Cartesian coordinate system and rotating the teeth around the z-axis so that the lingual side was parallel to the x-axis (e.g., Benazzi et al., 2012a). The crown outlines were projected onto the cervical plane, while the cervical outlines were represented by the contour of the section identified by the cervical plane itself. Both outlines (i.e., crown and cervical) were inscribed in a bounding box tangential to the most extreme points of the crowns to identify the mesio-distal (MD) and bucco-lingual (BL) diameters (Benazzi et al., 2011a; 2013a; Margherita et al., 2016).

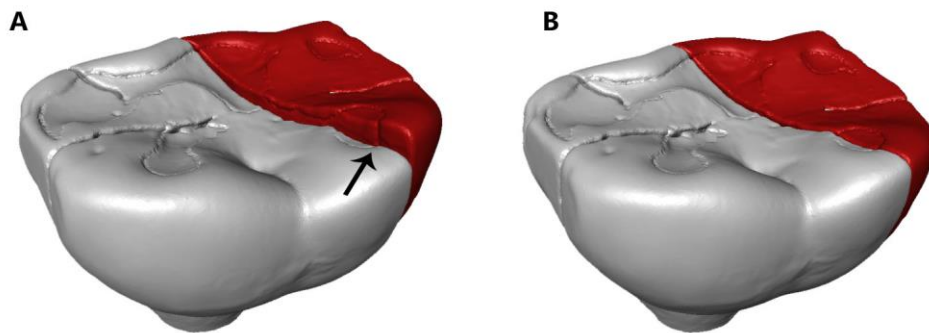


Figure S4. A) Original state of Dzu 2 (the arrow indicates the main crack); B) Virtual restoration of Dzu 2.

Moreover, for the deciduous molars we used crown (for Dzu 1, Dzu 2 and SATP5-5) and cervical outline analyses (for Dzu 2 and SATP5-5), following procedures in Benazzi et al. (2011b; 2012a) and Bailey et al. (2014). The outlines were imported in Rhino 4.0 Beta CAD environment (Robert McNeel and Associates, Seattle, WA), centered superimposing the centroids of their area,

represented by 16 pseudolandmarks for Dzu 2 and SATP5-5 (Benazzi et al., 2012a; 2014a) and by 24 pseudolandmarks for Dzu1 (Bailey et al., 2014) obtained by equiangularly spaced radial vectors out of the centroid, and scaled to unit centroid size (Benazzi et al., 2011b; 2012a; Bailey et al., 2014).

For the permanent teeth, we computed 3D enamel thickness following guidelines provided by Benazzi and colleagues (2014b). To quantify the 3D enamel thickness of the permanent teeth, the crown was separated from the root using the interpolated surface of the cervical line. We measured: the enamel volume (mm^3); the coronal dentine volume, which includes the volume of the crown pulp chamber (mm^3); and the enamel-dentine junction (EDJ) surface (mm^2). These measurements were used for the computation of both 3D average enamel thickness (3D AET = volume of enamel divided by the EDJ surface; in mm) and the 3D relative enamel thickness (3D RET = AET divided by the cubic root of dentine volume; scale-free) index.

Finally, in order to assess whether Dzu 1 and Dzu 2 belong to the same individual, both teeth were loaded in the Occusal Fingerprint Analyser (OFA) software (2008-2014 ZiLoX-IT GbR; www.for771.uni-bonn.de/for771-en/ofa). The software allows one model (i.e., Dzu 2) to be moved towards the antagonist (i.e., Dzu 1) along a defined pathway in order to analyse the collision of crown contacts. OFA software prevents the penetration of the models into one another and detects the occlusal contacts through collision detection, deflection and break free algorithms (for more details, see e.g., Benazzi et al., 2012b, 2013b, c, 2015, 2016; Kullmer et al., 2013; Fiorenza et al., 2015). Therefore, the colliding triangles of Dzu 1 and Dzu 2 during maximum intercuspation were detected and visualized to verify that they indeed belong to the same individual.

3. Results

3.1 Testing occlusal contacts between Dzu 1 and Dzu 2

Since Dzu 1 and Dzu 2 were retrieved from the same deposit, share a similar wear stage and root resorption, and represent antagonistic tooth classes (Rdm^2 and Rdm_2 , respectively), they might

belong to the same individual. However, only three occlusal contacts were detected during maximum intercuspation in the OFA software (SOM Fig. S5). Alternative solutions (e.g., moving Dzu 2 in slightly different positions), made the results even worse (results not shown). Overall, the few contact areas and the large gaps between the occlusal surfaces (Fig. S5) suggest the teeth do not belong to the same individual.

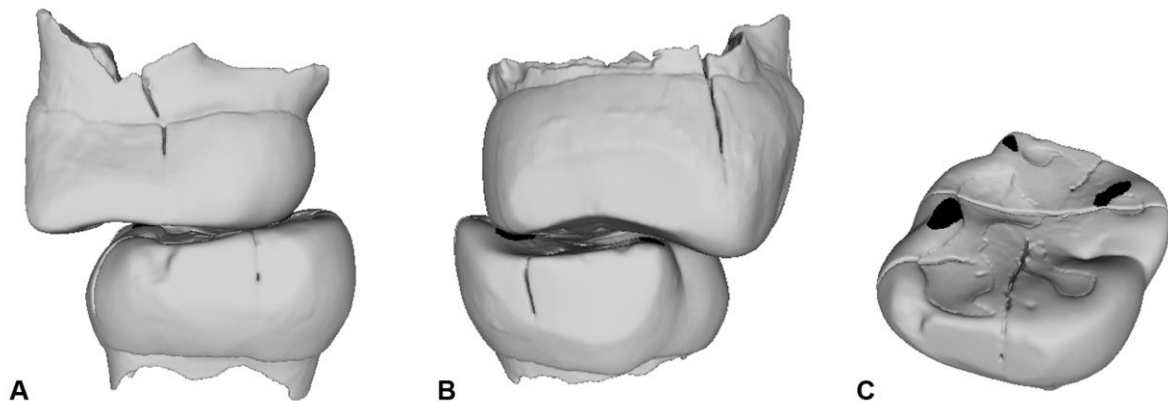


Figure S5. Collision detection for Dzu 1 (Rdm_1) and Dzu 2 (Rdm_2) in the Occlusal Fingerprint Analyser (OFA) software during maximum intercuspation (contact areas in black). A) mesial view; B) distal view; C) occlusal surface of Dzu 2 from mesio-lingual perspective.

3.2 Mandible

SATP5-5 shows several fractures. A fracture directed mesio-buccally/disto-lingually intersects the occlusal surface, from which a second fracture departs directed mesio-lingually. Another small fracture is visible in the protoconid cusp.

3.3 Metric comparison

The main metric dimensions of the SATP5 mandible are shown in SOM Table S1. The scatter plots between MD and BL diameters of the permanent teeth (see SOM Table S2 for the comparative sample used) are shown in SOM Figure S6.

Table S1.

Main metric dimensions of the SATP5 mandible.

Specimen/Sample	Age at death (years)	Corpus height at mental foramen (mm)	Corpus thickness at mental foramen (mm)	Robusticity Index at mental foramen^a	Source
SATP5	~ 6.0-7.0	21.4	10.5	49.0	Present study
<i>Neandertals</i>					
Gegant-5	~4.5-5.0	22.6	12.8	56.6	Quam et al., 2015
Palomas 49	~ 2.0	19.2	11.4	59.4	Walker et al., 2010
Barakai	~3.0	20.1	14.2	70.6	Mallegni and Trinkaus, 1997
Archi 1	~3.0	20.0	12.0	60.0	Mallegni and Trinkaus, 1997
Roc de Marsal	~3.0	17.0	12.7	74.7	Madre-Dupouy, 1992
Il Molare 1	~3.5	20.9	12.2	58.4	Mallegni and Trinkaus, 1997
Palomas 7	~4.0	21.3	12.7	59.6	Walker et al., 2010
La Chaise 13	~4.0	20.5	12.5	61.0	Mallegni and Trinkaus, 1997
Devil's Tower	~4.0	22.8	13.6	59.6	Mallegni and Trinkaus, 1997
Cova Negra (CN 7755)	~5.0	20.0	13.3	66.5	Arsuaga et al., 1989
Combe Grenal 1	~7.0	27.4	13.6	49.6	Garralda and Vandermeersch, 2000
<i>Modern Humans</i>					
Le Figuiet	~3.0	18.0	10.7	59.4	Billy, 1979

La Madeleine 4	~3.0	19.0	9.4	49.5	Heim, 1991
Lagar Velho	~4.5	20.5	11.5	56.1	Trinkaus, 2002
Skhul 1	~4.5	16.4	11.0	67.1	Mallegni and Trinkaus, 1997
Qafzeh 4	~6.0	26.3	14.2	54.0	Quam et al., 2015
Qafzeh 10	~6.0	24.2	13.3	55.0	Quam et al., 2015
Recent children (n=20)	2.0-5.0	17.2 ± 1.8	10.3 ± 1.0	60.4 ± 6.9	Madre-Dupouy, 1992

^a Calculated as (corpus thickness/corpus height) X 100.

Table S2.

Comparative sample (X indicates inclusion) of the P₃, P₄, M₁ and M₂ used for dental crown diameters (MD and BL) and three-dimensional (3D) enamel thickness analyses.

TAXON	Specimens	Tooth Class	Wear Stage	Diameters	Enamel Thickness
N	ABRISUARD_14_7	LM1	1	X	X
N	ABRISUARD_49	LM1	1	X	X
N	BDJ4C9	LM1	1	X	X
N	Engis	LM1	1	X	X
N	Krapina 52	LM1	1	X	X
N	Krapina 80	LM1	1	X	X
N	La Ferrasie 8	LM1	1	X	
N	Roc_de_Marsal	LM1	1	X	X
N	Taddeo 4 ^a	LM1	2	X	X
N	BD1	LM1	4	X	X
N	Krapina 53	LM1	3	X	X
N	Krapina 54	LM1	3	X	X
N	Krapina 55	LM1	3	X	X
N	Krapina 57	LM1	4	X	X
N	Krapina 58	LM1	4	X	X
N	Krapina 59	LM1	4	X	X
N	Le Moustier	LM1	4	X	X
N	Regourdou	LM1	4	X	X
N	St. Cesaire	LM1	4	X	X
N	Vindija_11_39	LM1	4	X	X
N	Weimer_Ehringsdorf	LM1	3	X	X
N	Scla_4A_1 ^b	LM1	3		X
N	Scla_4A_9 ^b	LM1	3		X
N	Kebara 2	LM1	5	X	X
EHS	AP_6242	LM1	2	X	X

EHS	AP_6277	LM1	1	X	X
EHS	Dar_Es_Sultane2_H4	LM1	4	X	X
EHS	Temara	LM1	4	X	X
UPHS	Villabruna	LM1	4		X
RHS	167_175_	LM1	2	X	X
RHS	213	LM1	2	X	X
RHS	M5	LM1	2	X	X
RHS	M6	LM1	2	X	X
RHS	R123	LM1	1	X	X
RHS	R488_274	LM1	2	X	X
RHS	R1160_440	LM1	2	X	X
RHS	R2602_1673	LM1	2	X	X
RHS	ULAC_1	LM1	3	X	X
RHS	ULAC_58	LM1	3	X	X
RHS	ULAC_74	LM1	4	X	X
RHS	ULAC_151	LM1	4	X	X
RHS	ULAC_536	LM1	4	X	X
RHS	ULAC_607	LM1	4	X	X
RHS	ULAC_790	LM1	4	X	X
RHS	ULAC_797	LM1	3	X	X
RHS	ULAC_801	LM1	3	X	X
N	Krapina 57	LM2	2	X	X
N	KRP_D1	LM2	2	X	X
N	LeMoustier	LM2	1	X	X
N	Krapina 54	LM2	1	X	X
N	Krapina_55	LM2	1	X	X
N	S36	LM2	2	X	X
N	SD540	LM2	1	X	X
N	Scladina 4A-1 ^b	LM2	2		X
N	Scladina 4A-9 ^b	LM2	1		X

N	Regourdou	LM2	3	X	X
N	Krapina_58	LM2	4	X	X
N	Krapina_59	LM2	3	X	X
N	St_Cesaire	LM2	4	X	X
EHS	AP_6282	LM2	2	X	X
EHS	Temara	LM2	2	X	X
EHS	Dar_Es_Sultane_H4	LM2	1	X	X
EHS	ElHarhoura	LM2	3	X	X
RHS	M145	LM2	3	X	X
RHS	167_I75	LM2	2	X	X
RHS	Belgian76a	LM2	2	X	X
RHS	M19_	LM2	2	X	X
RHS	M181	LM2	2	X	X
RHS	M190	LM2	2	X	X
RHS	M232	LM2	2	X	X
RHS	R115	LM2	2	X	X
RHS	R123	LM2	1	X	X
RHS	R258	LM2	2	X	X
N	Krapina_D34	LP3	2	X	X
N	Krapina_D111	LP3	1	X	X
N	Krapina_D114	LP3	1	X	X
N	Le_Moustier	LP3	1	X	X
N	Krapina_54	LP3	1	X	X
N	Krapina_52	LP3	1	X	X
N	Krapina_55	LP3	1	X	X
N	Scla_4A_6 ^b	LP3	1		X
N	KRAPINA_58	LP3	3	X	X
N	VI_11_45	LP3	3	X	X
EHS	Qafzeh_9	LP3	1	X	X
RHS	M14	LP3	2	X	X

RHS	M35	LP3	1	X	X
RHS	M36	LP3	1	X	X
RHS	ULAC_1	LP3	2	X	X
RHS	ULAC_13	LP3	1	X	X
RHS	ULAC_58	LP3	2	X	X
RHS	ULAC_151	LP3	1	X	X
RHS	ULAC_536	LP3	2	X	X
RHS	ULAC_790	LP3	2	X	X
RHS	ULAC_801	LP3	1	X	X
RHS	ULAC_806	LP3	1	X	X
RHS	ULAC_66	LP3	3	X	X
RHS	ULAC_74	LP3	3	X	X
RHS	ULAC_171	LP3	3	X	X
RHS	ULAC_522	LP3	3	X	X
N	KRP_D35	LP4	2	X	X
N	KRP_D50	LP4	1	X	X
N	KRP_D113	LP4	1	X	X
N	SD_763	LP4	1	X	X
N	CG_29	LP4	1	X	X
N	KRP_D118	LP4	1	X	X
N	Krapina_54	LP4	2	X	X
N	Krapina_52	LP4	1	X	X
N	Le_Moustier	LP4	1	X	X
N	Krapina_58	LP4	3	X	X
N	CG_VIII	LP4	4	X	X
N	Scla 4A-1 ^b	LP4	1		X
N	Scla 4A-9 ^b	LP4	1		X
EHS	Irhoud_3	LP4	1	X	X
EHS	Qafzeh_9	LP4	1	X	X
EHS	El_Harhoura	LP4	3	X	X

EHS	Temara	LP4	3	X	X
RHS	M7	LP4	1	X	X
RHS	M39	LP4	1	X	X
RHS	ULAC_1	LP4	2	X	X
RHS	ULAC_13	LP4	1	X	X
RHS	ULAC_74	LP4	2	X	X
RHS	ULAC_151	LP4	2	X	X
RHS	ULAC_790	LP4	2	X	X
RHS	ULAC_806	LP4	1	X	X
RHS	ULAC_171	LP4	3	X	X
RHS	ULAC_522	LP4	3	X	X
RHS	ULAC_799	LP4	3	X	X
RHS	ULAC_536	LP4	3	X	X

^a Benazzi et al., 2011c.

^b Benazzi et al., 2014c.

The values of the component of the 3D enamel thickness for the Satsurbliia permanent posterior teeth and the comparative sample are shown in Tables 3 and S3. For premolars and second molar at wear stage 1–2, Neandertals show significantly lower RET indices than RHS ($p < 0.01$; Table 3). In particular, the premolars show the largest differences between the two groups (i.e., Neandertals and *H. sapiens*). No significant differences were observed for the M₁ ($p = 0.507$). Even though the small EHS sample size prevents statistical analysis, the EHS means computed for all tooth classes are always closer to RHS than Neandertal.

When the 3D enamel thickness of Satsurbliia permanent teeth was compared with the RET mean values computed for Neandertals, EHS and RHS, the computed Z-scores are always closer to the *H. sapiens* means than to the Neandertal ones (Table 3).

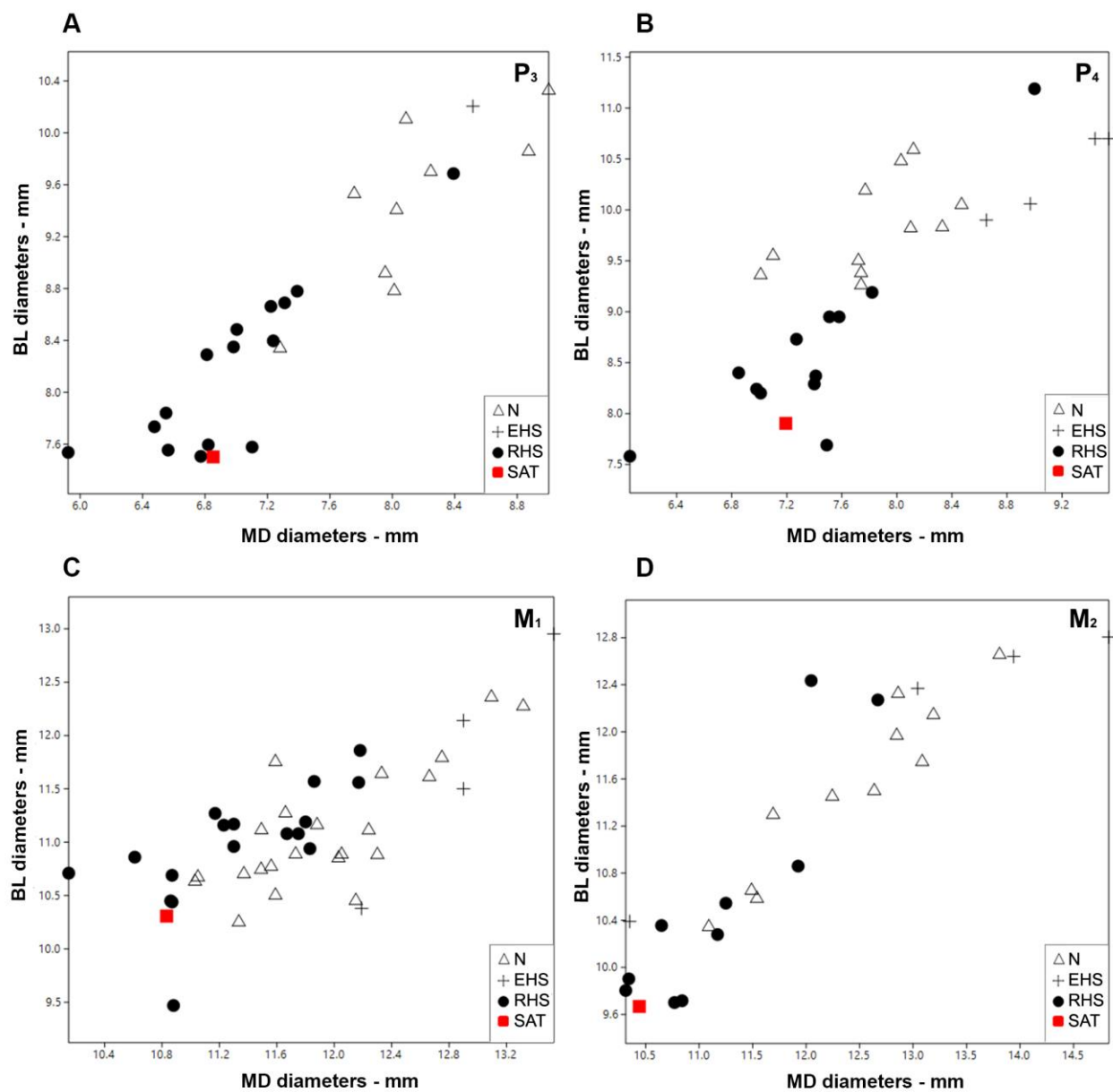


Figure S6. Scatter plot between MD and BL diameters of permanent teeth from Satsurblia cave. N = Neandertals; EHS = early *Homo sapiens*; RHS = recent *Homo sapiens*.

Table S3.Three-dimensional (3D) average enamel thickness (AET) and relative enamel thickness (RET).^a

Sample	Wear ^b	3D AET	Z-score	3D RET	Z-score
		Mean (SD/ <i>n</i>)		Mean (SD/ <i>n</i>)	
SATP5-3 (LP ₃)		1.17		26.75	
N	1-2	0.97 (0.08/8)	0.21	18.55 (1.60/8)	5.12
N	3	0.72 (0.09/2)		13.43 (2.14/2)	
EHS	1-2	1.3		24.76	
RHS	1-2	1.10 (0.13/11)	0.54	24.39 (2.38/11)	0.99
RHS	3	0.86 (0.06/4)	5.16	19.60 (0.93/4)	7.69
SATP5-4 (LP ₄)		1.61		41.46	
N	1-2	1.08 (0.09/11)	5.89	20.62 (2.37/11)	8.79
N	3	0.86 (0.02/2)		16.49 (0.19/2)	
EHS	1-2	1.39 (0.02/2)		25.23 (1.86/2)	
EHS	3	1.25 (0.07/2)		22.83 (8.37/2)	
RHS	1-2	1.20 (0.12/8)	3.42	25.69 (2.22/8)	7.10
RHS	3	1.16 (0.16/4)	2.81	25.01 (4.46/4)	3.69
SATP5-6 (LM ₁)		1.26		20.47	
N	1-2	1.22 (0.12/8)	0.33	18.61 (1.59/8)	1.17
N	3	1.08 (0.11/6)	1.64	15,86 (1.33/6)	3.47
N	4	0.81 (0.12/9)	3.75	12,21 (1.66/9)	4.97
EHS	1-2	1.23 (0.31/2)		19.64 (6.30/2)	
EHS	4	1.08 (0,14/2)		14.9 (1.66/2)	
RHS	1-2	1.23 (0,17/8)	0.18	20.17 (3.50/8)	0.29
RHS	3	1.04 (0.11/5)	2	16.16 (1.98/8)	2.18
RHS	4	0.90 (0.12/5)	3	14.30 (2.34/5)	2.64
SATP5-7 (LM ₂)		1.37		23.7	
N	1-2	1.18 (0.14/9)	1.36	17.42 (2.60/9)	2.41
N	3	0.94 (0.09/2)		13.88 (0.37/2)	
N	4	0.75 (0.19/2)		11.43 (3.78/2)	

EHS	1-2	1.41 (0.15/3)		22.10 (2.33/3)	
EHS	3	1.07 (0.15/2)		15.53 (0.97/2)	
RHS	1-2	1.34 (0.16/9)	0.19	21.61 (1.73/9)	1.20

^aSatsurbliia specimens are standardized to Z-scores of the Neandertal (N), early *H. sapiens* (EHS) and recent *Homo sapiens* (RHS) samples for different wear stages.

^b Molnar, 1971.

4. References

- Arsuaga, J.L., Gracia, A., Martínez, I., Bermúdez de Castro, J.M., Rosas, A., Villaverde, V., Fumanal, M.P., 1989. The human remains from Cova Negra (Valencia, Spain) and their place in European Pleistocene human evolution. *J. Hum. Evol.* 18, 55-92.
- Bailey, S.E., Benazzi, S., Souday, C., Astorino, C., Paul, K., Hublin, J.J., 2014. Taxonomic differences in deciduous upper second molar crown outlines of *Homo sapiens*, *Homo neanderthalensis* and *Homo erectus*. *J. Hum. Evol.* 72, 1–9.
- Bar-Yosef, O., Belfer-Cohen, A., Mesheviliani, T., Jakeli, N., Bar-Oz, G., Boaretto, E., Goldberg, P., Kvavadze, E., Matskevich, Z., 2011. Dzudzuana: an Upper Palaeolithic cave site in the Caucasus foothills (Georgia). *Antiquity* 85, 331–349.
- Benazzi, S., Coquerelle, M., Fiorenza, L., Bookstein, F., Katina, S., Kullmer, O., 2011a. Comparison of dental measurement systems for taxonomic assignment of first molars. *Am. J. Phys. Anthropol.* 144, 342-354.
- Benazzi, S., Douka, K., Fornai, C., Bauer, C.C., Kullmer, O., Svoboda, J.J., Pap, I.I., Mallegni, F., Bayle, P., Coquerelle, M., Condemi, S., Ronchitelli, A., Harvati, K., Weber, G.W., 2011b. Early dispersal of modern humans in Europe and implications for Neanderthal behaviour. *Nature* 479, 525-528.
- Benazzi, S., Viola, B., Kullmer, O., Fiorenza, L., Harvati, K., Paul, T., Gruppioni, G., Weber, G.W., Mallegni, F., 2011c. A reassessment of the Neanderthal teeth from Taddeo cave (southern Italy). *J. Hum. Evol.* 61, 377–387.

Benazzi, S., Fornai, C., Buti, L., Toussaint, M., Mallegni, F., Ricci, S., Gruppioni, G., Weber, G.W., Condemi, S., Ronchitelli, A., 2012a. Cervical and crown outline analysis of worn Neanderthal and modern human lower second deciduous molars. *Am. J. Phys. Anthropol.* 149, 537–546.

Benazzi, S., Kullmer, O., Grosse, I., Weber, G., 2012b. Brief communication: comparing loading scenarios in lower first molar supporting bone structure using 3D finite element analysis. *Am. J. Phys. Anthropol.* 147, 128-134.

Benazzi, S., Bailey, S.E., Mallegni, F., 2013a. Brief communication: A morphometric analysis of the Neanderthal upper second molar Leuca I. *Am. J. Phys. Anthropol.* 152, 300-305.

Benazzi, S., Nguyen, H.N., Schulz, D., Grosse, I.R., Gruppioni, G., Hublin, J.J., Kullmer, O., 2013b. The evolutionary paradox of tooth wear: simply destruction or inevitable adaptation? *PLOS ONE* 8, e62263.

Benazzi, S., Nguyen, H.N., Kullmer, O., Hublin, J.J., 2013c. Unravelling the functional biomechanics of dental features and tooth wear. *PLOS ONE* 8, e69990.

Benazzi, S., Bailey, S.E., Peresani, M., Mannino, M.A., Romandini, M., Richards, M.P., Hublin, J.J., 2014a. Middle Paleolithic and Uluzzian human remains from Fumane cave, Italy. *J. Hum. Evol.* 70, 61-68.

Benazzi, S., Panetta, D., Fornai, C., Toussaint, M., Gruppioni, G., Hublin, J.J., 2014b. Technical Note: Guidelines for the digital computation of 2D and 3D enamel thickness in hominoid teeth. *Am.*

J. Phys. Anthropol. 153, 305-313.

Benazzi, S., Toussaint, M., Hublin, J-J., 2014c. Enamel thickness in the Scladina Neandertal teeth. In: Toussaint, M., Bonjean, D. (Eds.), The Scladina I-4A Juvenile Neandertal. Liège: ERAUL, pp. 307 – 314.

Benazzi, S., Nguyen, H.N., Kullmer, O., Hublin, J.J., 2015. Exploring the biomechanics of taurodontism. J. Anat. 226, 180-188.

Benazzi, S., Nguyen, H.N., Kullmer, O., Kupczik, K., 2016. Dynamic modelling of tooth deformation using occlusal kinematics and finite element analysis. PLOS ONE 11, e0152663.

Billy, G., 1979. L'enfant Madgalénien de la Grotte du Figuier (Ardèche). L'Anthropologie 83, 223-252.

Buikstra, J.E., Ubelaker, D.H. (Eds.), 1994. Standards for data collection from human skeletal remains: proceedings of a seminar at the Field Museum of Natural History. Arkansas Archeological Survey Research Series No. 44.

Fiorenza, L., Nguyen, H.N., Benazzi, S., 2015. Stress distribution and molar macrowear in *Pongo pygmaeus*: A new approach through finite element and occlusal fingerprint analyses. Hum. Evol. 30, 215-226.

Garralda, M., Vandermeersch, B., 2000. Les Néandertaliens de la Grotte de Combe-Grenal (Domme, France). Paleo 12, 213-259.

Heim, J.L., 1991. L'enfant Magdalénien de la Madeleine. *L'Anthropologie* 95, 611-638.

Kullmer, O., Benazzi, S., Schulz, D., Gunz, P., Kordos, L., Begun, D.R., 2013. Dental arch restoration using tooth macrowear patterns with application to *Rudapithecus hungaricus*, from the late Miocene of Rudabánya, Hungary. *J. Hum. Evol.* 64, 151-160.

Kvavadze, E., Bar-Yosef, O., Belfer-Cohen, A., Boaretto, E., Jakeli, N., Matskevich, Z., Meshveliani, T., 2009. 30 000-year-old wild flax fibers. *Science* 325, 1359.

Madre-Dupouy, M., 1992. L'enfant du Roc de Marsal: Etude Analytique et Comparative. CNRS, Paris.

Mallegni, F., Trinkaus, E., 1997. A reconsideration of the Archi 1 Neandertal mandible. *J. Hum. Evol.* 33, 651-668.

Margherita, C., Talamo, S., Wiltchke-Schrotta, K., Senck, S., Oxilia, G., Sorrentino, R., Mancuso, G., Gruppioni, G., Lindner, R., Hublin, J.J., Benazzi, S., 2016. A reassessment of the presumed Torrener Bärenhöhle's Paleolithic human tooth. *J. Hum. Evol.* 93, 120-125.

Molnar, S., 1971. Human tooth wear, tooth function and cultural variability. *Am. J. Phys. Anthropol.* 34, 175-189.

Panetta, D., Belcari, N., Del Guerra, A., Bartolomei, A., Salvadori, P.A., 2012. Analysis of image sharpness reproducibility on a novel engineered micro-CT scanner with variable geometry and embedded recalibration software. *Phys. Medica* 28, 166-173.

Pinhasi, R., Meshveliani, T., Matskevich, Z., Bar-Oz, G., Weissbrod, L., Miller, C.E., Wilkinson, K., Lordkipanidze, D., Jakeli, N., Kvavadze, E., Higham, T.F.G., Belfer-Cohen, A., 2014.

Satsurbliia: New insights of human response and survival across the Last Glacial Maximum in the southern Caucasus. *PLOS ONE* 9, e111271.

Quam, R., Sanz, M., Daura, J., Robson Brown, K., García-González, R., Rodríguez, L., Dawson, H., Rodríguez, R.F., Gómez, S., Villaescusa, L., Rubio, A., Yagüe, A., Ortega Martínez, M.C., Fullola, J.M., Zilhão, J., Arsuaga, J.L., 2015. The Neandertals of northeastern Iberia: New remains from the Cova del Gegant (Sitges, Barcelona). *J. Hum. Evol.* 81, 13-28.

Rosas, A., Bermúdez de Castro, J.M., 1999. The ATD6-5 mandibular specimen from Gran Dolina (Atapuerca, Spain). Morphological study and phylogenetic implications. *J. Hum. Evol.* 37, 567-590.

Trinkaus, E., Ruff, C., Esteves, F., Santos-Coelho, J., Silva, M., Mendonça, M., 2002. The upper limb remains. In: Zilhão, J., Trinkaus, E. (Eds.), *Portrait of the Artist as a Child: The Gravettian Human Skeleton from the Abrigo do Lagar Velho and its Archeological Context*. Instituto Português de Arqueologia, Lisboa, pp. 466-488.

Walker, M.J., Lombardi, A.V., Zapata, J., Trinkaus, E., 2010. Neandertal mandibles from the Sima de las Palomas del Cabezo Gordo, Murcia, southeastern Spain. *Am. J. Phys. Anthropol.* 142, 261-272.